Title

Fatty acid bioaccessibility and structural breakdown from in vitro digestion of almond particles.

Journal

Food & function, 10(8)

ISSN

2042-6496

Authors

Swackhamer, Clay
Zhang, Zhichao
Taha, Ameer Y
et al.

Publication Date

2019-08-01

DOI

10.1039/c9fo00789j

Peer reviewed

Food & Function

PAPER

View Article Online
View Journal

Cite this: DOI: 10.1039/c9fo00789j

Fatty acid bioaccessibility and structural breakdown from *in vitro* digestion of almond particles†

Clay Swackhamer,[a] Zhichao Zhang,[b] Ameer Y. Taha[b] and Gail M. Bornhorst *[a,b,c]

Received 16th April 2019,
Accepted 19th July 2019

DOI: 10.1039/c9fo00789j

rsc.li/food-function

Previous studies have shown that the size of almond particles influences lipid bioaccessibility during digestion. However, the extent of structural breakdown of almond particles during gastric digestion and its impact on lipid bioaccessibility is unclear. In this study, *in vitro* digestion of almond particles was conducted using a dynamic model (Human Gastric Simulator) and a static model (shaking water bath). Structural breakdown of particles during the gastric phase occurred only in the Human Gastric Simulator, as evidenced by a reduction in particle size (15.89 ± 0.68 mm^2 to 12.19 ± 1.29 mm^2, $p < 0.05$). Fatty acid bioaccessibility at the end of the gastric phase was greater in the Human Gastric Simulator than in the shaking water bath (6.55 ± 0.85% *vs.* 4.54 ± 0.36%, $p < 0.01$). Results showed that the *in vitro* model of digestion which included peristaltic contractions (Human Gastric Simulator) led to breakdown of almond particles during gastric digestion which increased fatty acid bioaccessibility.

Introduction

Almonds have high lipid content (44–61 g per 100 g whole almond).[1] However, previous studies have shown that the bioaccessibility of lipids from almond particles is limited by encapsulation within intact almond cells, which resist degradation in the human digestive system.[2–5] In accordance with previous researchers, bioaccessibility was defined in this study as the proportion of lipid released from the almond matrix into the aqueous digestive environment.[6,7] Understanding the factors that influence bioaccessibility of lipids during digestion of almonds has implications for clinical nutrition in view of studies showing that the limited bioaccessibility of lipids from almonds reduces postprandial lipemia[8] and metabolizable energy.[9,10] Limited lipid bioaccessibility from almonds and other nuts has also been linked to improved metabolic markers in type 2 diabetes,[11] cardiovascular disease,[12,13] and obesity.[14]

Previous studies have investigated the digestion of almonds using both *in vitro*[2,3,5,15] and *in vivo*[8–10,16–19] methods, and it has been observed that smaller particles led to higher lipid bioaccessibility than larger particles.[2,3,19] Additionally, researchers have reported size reduction of peanut particles during *in vitro* gastric digestion in a model that simulated the motility of the human stomach.[20] The relationship between particle size and fatty acid bioaccessibility in the human digestive system has been described using a mathematical model,[6] but an assumption was that particle size was constant throughout the digestion. Size reduction of almond particles during gastric digestion has been observed in studies using the growing pig as a model for the adult human, but was not directly linked to lipid bioaccessibility.[21–23] This points to the need for more data on the breakdown of almond particles during digestion to clarify the relationship between particle breakdown and lipid bioaccessibility. However, static *in vitro* models of human digestion do not reproduce the peristaltic motion of the stomach[24] and thus may not lead to particle breakdown as it occurs *in vivo*. Thus, an *in vitro* model of gastric digestion that included peristaltic contractions, the Human Gastric Simulator (HGS), was used to assess whether peristaltic motion contributed to particle breakdown and lipid bioaccessibility during simulated gastric digestion.

Briefly, the HGS includes a flexible plastic liner which holds the food and simulated gastric juice. Simulated peristaltic contractions are applied to the HGS using rollers, and temperature and pH can be controlled to appropriately simulate the conditions inside the human stomach. An in-depth comparison of the HGS with other dynamic, *in vitro* models of human digestion has been described in a recent review.[25] A similar *in vitro* model is the Dynamic Gastric Model, which was used by previous researchers for *in vitro* digestion of almond particles.[15]

[a]*Department of Biological and Agricultural Engineering, University of California, Davis, USA. E-mail: gbornhorst@ucdavis.edu*
[b]*Department of Food Science and Technology, University of California, Davis, USA*
[c]*Riddet Institute, Palmerston North, New Zealand*

†Electronic supplementary information (ESI) available. See DOI: 10.1039/c9fo00789j

This model includes simulated peristaltic waves, which are applied by water pressure, in addition to pH and temperature control. Another previously reported *in vitro* model of human digestion is the TIM model,[26,27] which also includes simulated peristaltic contractions applied by water pressure. Previous researchers also used a dynamic *in vitro* model of gastric digestion to show that peanut particles experienced size reduction during simulated gastric digestion.[20] This model consists of a ball-shaped probe, actuated by a texture analyzer, which was used to gently mix the contents of a vessel containing the food subjected to *in vitro* digestion.[20]

The objective of this study was to determine whether digestion of almond particles using an *in vitro* model with peristaltic contractions (HGS) led to particle breakdown and whether this affected fatty acid bioaccessibility. This was investigated using *in vitro* digestion of almond particles in either the HGS or a shaking water bath using identical simulated digestive juices. The second objective of the study was to determine the effect of simulated gastric and intestinal juices on the bioaccessibility of fatty acids from almond particles. This was done by digesting almond particles in a shaking water bath model using simulated gastric and intestinal juices or with only pH-adjusted water. Identifying the factors that affect fatty acid bioaccessibility could have implications for design of appropriate models for simulating human digestion and could assist in the development of functional foods for targeted fatty acid bioaccessibility.

Materials and methods

Raw materials

Whole, raw nonpareil almonds were generously donated by the Almond Board of California. Almonds had size of 22.69 ± 1.13 mm, 12.72 ± 0.43 mm, 7.82 ± 0.62 mm (length ± std, width ± std, height ± std, n = 20 almonds were subjected to measurement with a digital caliper). Almonds were prepared for *in vitro* digestions by grinding in a food processor (Black & Decker FP2500B, Towson MD). Particles between 2 mm and 4 mm in size were obtained by sieving (WS Tyler, Mentor OH). This size range was chosen to approximate the size of almond particles in a masticated bolus at the point of swallow.[28,29] The resulting almond particles, of a size similar to those from mastication *in vivo*, were then used for *in vitro* digestions. Almond particles produced using the food processor were prepared fresh each day before conducting *in vitro* digestions.

Digestive juice formulation

Digestive juices were prepared using a previously described method[30,31] (Table 1). Water used for digestive juices was obtained from a Milli-Q Water Purification System (Merck Millipore, Billerica, MA, USA). Saliva has been found to be important for the *in vitro* digestion of starchy foods due to the prevalence of salivary α-amylase, however, almonds have little to no starch content.[1,32] Saliva was not used in this study in accordance with previous *in vitro* digestion research on almond particles.[2,3] Enzymes were added to simulated gastric and intestinal juices to reflect their activity *in vivo*, as identified by the INFOGEST international consensus protocol[33] (Table 1). Amano Lipase A was used due to its resistance to pepsin[34,35] and for agreement with previous *in vitro* digestion research.[36,37] However, it is acknowledged that the stereospecificity of this lipase is not well described,[35] which could affect the results of fatty acid bioaccessibility.

Shaking water bath model

Shaking water bath model with simulated gastric and intestinal juices. Digestions in the shaking water bath were conducted by adding simulated gastric juice (Table 1, prewarmed to 37 °C) to almond particles in a ratio of 5 mL simulated gastric juice to 1 g almond particles. After adding simulated gastric juice, the pH was recorded (Accumet AE150, Thermo-Fisher, Waltham, MA), and the bottle containing almond particles and simulated gastric juice was placed in a shaking water bath (Thermo-Fisher 2872, Waltham, MA) at 37 °C and 100 rpm. After 60 min elapsed time, the pH was adjusted to 3 ± 0.1 and after 120 min to 2 ± 0.1 to simulate the dynamic pH profile in the human stomach after consumption of a meal.[35,38] After 180 min, the intestinal phase was initiated by adding simulated intestinal juice (Table 1, prewarmed to 37 °C) in a 1 : 1 (v/v) ratio with the simulated gastric juice that

Table 1 Composition of simulated digestive juices[30,31,33]

	Component	Supplier	Concentration in simulated digestive juice (mg mL^{-1})	Activity in simulated digestive juice
Simulated gastric juice (pH = 1.8)	Pepsin (300 U mg^{-1})	MP Biomedicals CAS: 9001-75-6	6.67	2000 U mL^{-1}
	Gastric mucin (porcine stomach – Type II)	Sigma-Aldrich CAS: 84082-64-4	1.50	—
	Amano Lipase A (120 000 U g^{-1})	Sigma-Aldrich CAS: 9001-62-1	3.33	40 U mL^{-1}
	NaCl	Fisher Scientific CAS: 7647-14-5	8.78	—
Simulated intestinal juice (pH = 7)	Pancreatin (8X USP)	Sigma-Aldrich CAS: 8049-47-6	9.60	100 TAME units per mL (for trypsin)
	Bile extract	Sigma-Aldrich CAS: 8008-63-7	10.00	—
	$NaHCO_3$	Sigma-Aldrich CAS: 144-55-8	16.80	—

was added to begin the gastric phase, and pH was adjusted to 7 ± 0.1. After 60 min simulated intestinal digestion (240 min total), pH was readjusted to 7 ± 0.1. After 120 min simulated intestinal digestion (300 min total) pH was again adjusted to 7 ± 0.1. All pH adjustments were made using 3 M HCl or 3 M NaOH. This pH adjustment protocol was used to resemble the pH in the digestive system after consumption of a meal of almonds *in vivo*.[39]

Samples were collected for analysis at 8 timepoints (gastric: 1, 5, 15, 30, 180 min, intestinal: 185, 195, 360 min total time). For any timepoint, the entire contents of the bottle in the shaking water bath were collected for analysis (Fig. 1). The digesta was collected by pouring through a kitchen sieve (aperture size ~0.5 mm) to separate the solid phase (almond particles) from the liquid phase. All digestions were completed in triplicate.

Shaking water bath model with only pH-adjusted water. Digestions were also conducted in the shaking water bath model using only pH-adjusted water. The gastric phase was initiated by adding water (pH = 1.8 ± 0.1) to almond particles in a ratio of 5 mL acidified water to 1 g almond particles. At the end of the gastric phase, water (pH = 7 ± 0.1) was added in a 1 : 1 (v/v) ratio with the acidified water that had been added to begin the gastric phase. Adjustments of pH and sample collection were conducted as described previously.

Human gastric simulator model using simulated digestive juices

The Human Gastric Simulator (HGS) is a single-chamber model of human gastric digestion that simulates peristaltic contractions using mechanical rollers on a flexible plastic liner containing food and simulated gastric juice.[25,40] Digestions in the HGS were conducted by adding simulated gastric juice to almond particles in the same ratio as was used for the shaking water bath. During the gastric phase, the contents of the HGS were subjected to peristaltic contractions at a frequency of 3 contractions per minute.[41] As the HGS was used to test the impact of peristaltic motion on the breakdown of almond particles in comparison to the shaking water bath model, no secretions were added during the digestion to keep the ratio of solid particles to simulated gastric juice constant for both models. At the end of the gastric phase the contents of the HGS were transferred to a bottle, simulated intestinal juice was added in a 1 : 1 (v/v) ratio with the simulated gastric juice that was added to begin the gastric phase, and the bottle was transferred to the shaking water bath at 37 °C. The pH in the HGS was adjusted in the same way as for digestions using the shaking water bath. Sampling was conducted by removing the entire contents of the HGS bag (during the gastric phase) or bottle (during the intestinal phase). Solid and liquid phases were separated by sieving in the same way as was done for digestions using the shaking water bath. Each aliquot of almond particles subjected to *in vitro* digestion in the HGS was ~60 g, and each aliquot used for *in vitro* digestion in the shaking water bath was ~15 g.

Analysis of liquid phase

After separation of solid and liquid phases by sieving, the liquid phase was homogenized for one minute at 10 000 rpm (Ultra Turrax T18 digital with S18N-19G disperser, IKA Works, Wilmington, NC). °Brix of the homogenized liquid phase was measured in triplicate using a digital refractometer (HI 96800, Hanna Instruments, Woonsocket, RI), and expressed as the measured value minus the °Brix of the appropriate blank simulated digestive juice. Remaining homogenized digesta was promptly frozen at −20 °C and stored until fatty acid analysis could be completed (less than one month). It has been found that storage of lipids from foods at this temperature for short periods of time does not lead to significant fatty acid oxidation.[42,43] No antioxidant was added to the samples during short-term storage, in accordance with previous research on the bioaccessibility of fatty acids from almonds.[2]

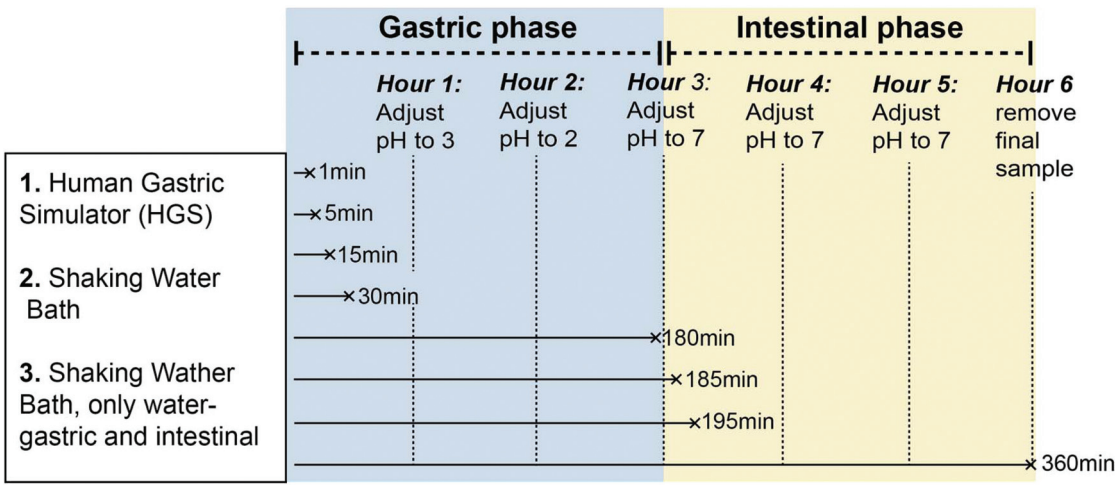

Fig. 1 The gastric phase of digestion was conducted in either the Human Gastric Simulator (HGS) or a shaking water bath. After the gastric phase, the intestinal digestion was always conducted in the shaking water bath. All digestions were conducted at 37 °C.

Although a small amount of fatty acids could have been lost during storage or sample preparation through formation of oxidized products, previous researchers have determined that there was no statistically significant increase in markers of lipid oxidation during storage of food samples at −20 °C for less than one month.[44]

Fatty acid extraction and preparation. Fatty acids were extracted from liquid digesta and analyzed using gas chromatography with flame ionization detection (GC-FID). The objective was to determine the amount of fatty acids that had left the almond matrix and entered the liquid phase, as a percentage of those initially present in the almonds. Fatty acids were extracted from liquid digesta using the Folch method, a standard method for extraction of total lipids from foods and digesta.[45–47] Briefly, 0.5 mL of homogenized digesta was combined with 2 mL of a 2 : 1 chloroform : methanol (v/v) solution containing triheptadecanoin internal standard (Nu-Chek Inc., Elysian MN). The mixture was vortexed and then centrifuged at 458*g* for 10 min (Allegra 6 centrifuge with GH-3.8A rotor, Beckman Coulter, Palo Alto CA). The chloroform layer was transferred to a new test tube. The extraction was repeated a second time and the chloroform layers were combined and then evaporated under nitrogen (Reacti-Vap TS-18826, Thermo-Fisher, Waltham, MA). Dried extracts were reconstituted using 400 μL toluene, 3 mL methanol and 600 μL of a 3% HCl in methanol (v/v) solution, and vortexed. The 3% methanolic HCl solution was prepared by diluting a 37% HCl solution (ACS reagent, 37%, Sigma-Aldrich, St. Louis, MO, USA; Cat #320331) to 8% in methanol. Samples were placed in a heating block at 90 °C for 60 min for transesterification, obtaining fatty acid methyl esters. After cooling, 1 mL deionized water and 1 mL hexane were added and vortexed. After allowing 15 min for phase separation, the hexane layer was transferred to a microcentrifuge tube containing 450 μL deionized water which was centrifuged at 16 627*g* for 2 min at 4 °C (5430R Eppendorf micro-centrifuge with FA-45-24-11 rotor, Fisher Scientific, Waltham MA). After centrifuging, the hexane layer was transferred to a new microcentrifuge tube, evaporated under nitrogen, and reconstituted in 100 μL hexane for analysis using GC-FID.

GC-FID analysis of fatty acids. Samples were run on a PerkinElmer Clarus 500 GC system (PerkinElmer, Shelton, CT) with a FFAP column (30 m × 0.25 mm inner diameter, 0.25 μm film thickness; Agilent Technologies, Santa Clara, CA) and flame ionization detector sampling at 1.25 Hz. The injector temperature was 240 °C and the detector temperature was 300 °C. The oven temperature was held at 80 °C for 2 min, then increased by 10 °C per min to 185 °C at the time of injection, and then increased to 240 °C at 5 °C min^{-1} and held at 240 °C for 13 min. Total run time was 36.5 minutes. The carrier gas was helium at a flow rate of 1.3 mL min^{-1}. The injection volume was 1 μL and the split ratio was 10 : 1. A mixture containing 29 fatty acid methyl ester standards was run separately from the experimental samples and used to identify individual fatty acids based on their retention times.[48] Fatty acid concentrations in the liquid digesta were determined by comparison of peak areas to the peak from the triheptadecanoin internal standard. Fatty acid analysis was also performed on samples of simulated gastric and intestinal juice, and the fatty acid content of experimental samples of almond digesta was adjusted by subtraction of the appropriate blank. Total bioaccessible fatty acid in the digesta was defined as the sum of palmitic acid (C16:0), oleic acid (C18:1), and linoleic acid (C18:2) extracted from 0.5 mL digesta, multiplied by the total volume of digesta that was collected. It was determined that these three fatty acids constituted >98% of the total fatty acid content of the whole almonds, which is in agreement with a previous analysis of California-grown almonds.[32]

Analysis of solid phase

After collection of a digestion timepoint and separation of solid and liquid phases by sieving, solid almond particles were drained on the sieve for 15 min. For each timepoint, 5 aliquots of digested particles were randomly selected from the drained solids and used for moisture content analysis. Moisture content was determined gravimetrically using AOAC Official Method 925.4061 by drying at 110 °C to constant weight. Remaining almond particles were used for particle size analysis as well as for Scanning Electron Microscopy.

Particle size analysis. The initial size of almond particles subjected to *in vitro* digestion was controlled (2 mm–4 mm), thus, the objective of the particle size analysis was to quantify size reduction of particles that occurred during simulated gastric or intestinal digestion. An image analysis procedure developed by previous researchers to quantify the size distribution of fractured almond particles was used in this study to measure the size of almond particles.[9] Minor modifications were made to adapt the image analysis procedure for this study. Briefly, 6 g almond particles were arranged onto Petri dishes to prevent overlap. Petri dishes were illuminated from beneath using a lightbox (AGPtek HL0163, color temperature 6000°K). A geometrical reference (ABFO no. 2 photomacrographic standard reference scale) was included in all images for spatial calibration. One image of each dish was captured using a Canon EOS Rebel SL1 digital camera (18-megapixel, APS-C CMOS sensor, Canon USA, San Jose, CA). The camera settings were: no flash, 35 mm focal length, aperture F8.0, ISO 100, and shutter speed 0.1 second, 47 mm distance to the particles. The camera was triggered using a computer interface to reduce disturbances in focus. Images were analyzed using MATLAB R2018b (MathWorks, Natick MA). The number of particles per gram of dry solids was defined as the number of particles that were enumerated during image analysis divided by the dry mass of particles subjected to image analysis (3.68 ± 0.62 g). Particle size analysis was conducted by fitting the cumulative area percentage of the particles to the Rosin–Rammler model (eqn (1)).

$$C_{\text{area}} = 1 - \exp\left(-\left(\frac{x}{x_{50}}\right)^{b} \ln(2)\right) \quad (1)$$

where: C_{area} is cumulative area percentage of each particle (0% to 100%), x_{50} = median particle area (mm^2), and b is the distribution breadth constant (dimensionless), where larger b values represent a narrower distribution spread. This model

has previously been used to describe the size of solid food particles as determined by image analysis.[9,22]

Scanning electron microscopy. Scanning electron microscopy (SEM) was conducted on almond particles digested for 180 minutes in the HGS as well as undigested almond particles as a control. Images were obtained using a previously described method.[49,50] Briefly, almond particles were mounted on double-sided carbon tape and sputter coated in gold. Micrographs were obtained using a scanning electron microscope (Quattro S, Thermo-Fisher, Waltham, MA) in high vacuum mode with acceleration voltage of 5 kV.

Almond composition

The fatty acid content of whole almonds was determined using Folch extraction as well as by direct acid extraction. For both methods almonds were ground in a mortar and pestle. Folch extraction was conducted on 10 mg almond powder as previously described. Direct acid extraction was carried out on 10 mg almond powder by adding 3 mL 3% HCl in methanol, prepared as described previously, then following the rest of the steps described previously starting with addition of 400 μL toluene. Composition data from direct acid extraction and Folch extraction are shown in ESI Table 1.† It was determined that direct acid extraction yielded more fatty acid and was therefore used to establish the initial fatty acid content of almonds. Fatty acid bioaccessibility at different timepoints during the digestion was expressed by dividing total fatty acid in the liquid digesta (g bioaccessible fatty acid) by the fatty acid in the undigested almonds (g initial fatty acid).

Statistical analysis

Statistical analysis was conducted using SAS Enterprise Guide 7.1 (SAS Institute, Cary NC). Two factor analysis of variance (ANOVA) was used to determine the influence of digestion model (HGS, shaking water bath-gastric fluids, or shaking water bath-only pH adjusted water), digestion time (1, 5, 15, 30, 180, 185, 195, or 360 min) and their interaction on fatty acid bioaccessibility, Rosin–Rammler x_{50}, Rosin–Rammler b, particles per gram of dry solids, moisture content of digesta, and °Brix of digesta. Homogeneity of variance was assessed using the Brown–Forsythe test, and normality of the residuals was assessed using a qq plot. Remediation was necessary for ° Brix and particles per gram of dry solids and was conducted using the Box–Cox transformation (lambda values 0.33 and −1.83, respectively). When the F value for the overall model was found to be significant ($p < 0.05$), post-hoc tests were conducted using Tukey's HSD and significance was detected for $p < 0.05$. All results are presented as mean ± standard deviation.

Results

Fatty acid bioaccessibility

Total bioaccessible fatty acid (%) was significantly influenced by digestion model, digestion time, and their interaction ($p < 0.01$, Fig. 2). Within each model, total bioaccessible fatty acid (%) significantly increased over time ($p < 0.01$). After the end of the gastric phase (180 min) the total fatty acid bioaccessibility was greater in the HGS (6.55 ± 0.85%) than in the shaking water bath model with gastric juice (4.54 ± 0.36%), $p < 0.05$. However, total fatty acid bioaccessibility at the end of the gastric phase in the shaking water bath model with gastric juice (4.54 ± 0.36%) was not significantly different than in the shaking water bath model with only pH adjusted water (4.38 ± 0.37%), $p > 0.05$. Thus, total fatty acid bioaccessibility at the end of the gastric phase was significantly higher in the model with peristaltic motion (HGS) than in the models that lacked peristaltic motion (shaking water bath model with gastric juice, shaking water bath model with only pH adjusted water).

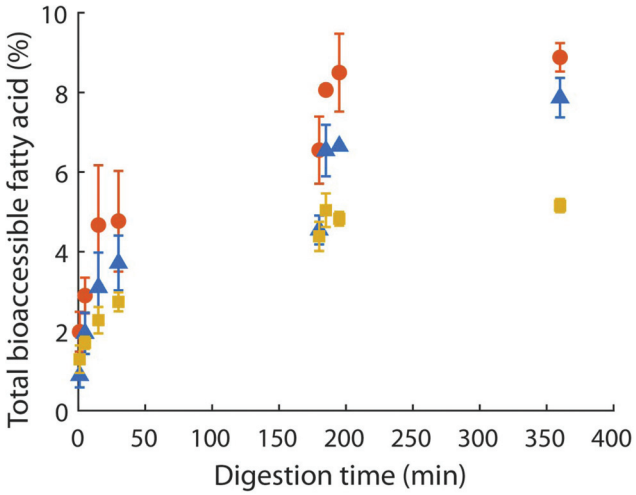

Fig. 2 Total percent fatty acid bioaccessibility in the Human Gastric Simulator (●), shaking water bath (▲), and shaking water bath with only pH-adjusted water (■) models. All points represent the mean (n = 3) ± standard deviation.

After the end of the simulated gastric and intestinal digestion, total fatty acid bioaccessibility was not significantly different in the HGS (8.88 ± 0.36%) than in the shaking water bath model with gastric juices (7.87 ± 0.49%), $p > 0.05$. However, total fatty acid bioaccessibility in the HGS as well as the shaking water bath model with gastric juices were both significantly higher than fatty acid bioaccessibility in the shaking water bath model with only pH adjusted water (5.15 ± 0.17%), $p < 0.05$. Thus, at the end of the intestinal phase total fatty acid bioaccessibility was significantly higher in the models with simulated gastric and intestinal juices (HGS and shaking water bath model with gastric and intestinal juices) than in the model with only pH adjusted water (shaking water bath model with only pH adjusted water).

The percent bioaccessibility of individual fatty acids (C16:0, C18:1, C18:2, Table 2) was significantly influenced by the digestion model, digestion time, and their interaction ($p < 0.01$). The percent bioaccessibility of each individual fatty acid increased with time in all three digestion models ($p < 0.01$,

Table 2 Bioaccessible fatty acid in liquid digesta as percentage of initial fatty acid content of almonds. All values are means (n = 3) ± standard deviation. Values in each column with no letter in common (abc) represent significant differences ($p < 0.05$) within a certain model across different digestion times. Values in each row with no letter in common (xyz) represent significant differences ($p < 0.05$) at a certain digestion time across the gastric digestion models for each fatty acid. If no letter is listed, there were no significant differences

	C16:0 (% bioaccessible)			C18:1 (% bioaccessible)			C18:2 (% bioaccessible)		
Time (min)	HGS	Shaking water bath	Shaking water bath with only pH adjusted water	HGS	Shaking water bath	Shaking water bath with only pH adjusted water	HGS	Shaking water bath	Shaking water bath with only pH adjusted water
1	1.56 ± 0.86^{d}	0.96 ± 0.3^{d}	1.27 ± 0.34^{c}	1.85 ± 0.36^{d}	0.84 ± 0.29^{d}	1.24 ± 0.33^{b}	1.95 ± 0.64^{d}	1.01 ± 0.33^{d}	1.49 ± 0.40^{b}
5	2.87 ± 0.42^{d}	1.95 ± 0.48^{cd}	1.65 ± 0.16^{c}	2.79 ± 0.44^{d}	1.87 ± 0.51^{cd}	1.64 ± 0.15^{b}	3.25 ± 0.50^{d}	2.2 ± 0.57^{c}	1.95 ± 0.17^{b}
15	$4.57 \pm 1.47^{c,x}$	$3.05 \pm 0.80^{bc,y}$	$2.20 \pm 0.32^{c,y}$	$4.48 \pm 1.44^{c,x}$	$2.99 \pm 0.87^{bc,y}$	$2.19 \pm 0.32^{b,y}$	$5.31 \pm 1.72^{c,x}$	$3.5 \pm 0.94^{bc,y}$	$2.59 \pm 0.38^{b,y}$
30	$4.68 \pm 1.22^{c,x}$	$3.63 \pm 0.64^{b,xy}$	$2.64 \pm 0.24^{bc,y}$	$4.57 \pm 1.21^{c,x}$	$3.57 \pm 0.67^{b,xy}$	$2.64 \pm 0.23^{b,y}$	$5.43 \pm 1.47^{c,x}$	$4.21 \pm 0.76^{b,xy}$	$3.12 \pm 0.28^{b,y}$
180	$6.38 \pm 0.83^{b,x}$	$4.43 \pm 0.38^{b,y}$	$4.18 \pm 0.30^{ab,y}$	$6.30 \pm 0.82^{b,x}$	$4.37 \pm 0.34^{b,y}$	$4.21 \pm 0.36^{a,y}$	$7.44 \pm 0.94^{b,x}$	$5.14 \pm 0.43^{b,y}$	$5.02 \pm 0.41^{a,y}$
185	$8.23 \pm 0.22^{a,x}$	$6.88 \pm 0.87^{a,y}$	$4.83 \pm 0.43^{a,z}$	$7.74 \pm 0.13^{ab,x}$	$6.31 \pm 0.57^{a,y}$	$4.85 \pm 0.40^{a,z}$	$9.08 \pm 0.15^{ab,x}$	$7.2 \pm 0.84^{a,y}$	$5.72 \pm 0.50^{a,z}$
195	$8.63 \pm 0.93^{a,x}$	$7.04 \pm 0.24^{a,y}$	$4.63 \pm 0.18^{a,z}$	$8.18 \pm 0.95^{a,x}$	$6.41 \pm 0.05^{a,y}$	$4.65 \pm 0.16^{a,z}$	$9.52 \pm 1.09^{a,x}$	$7.35 \pm 0.10^{a,y}$	$5.48 \pm 0.23^{a,z}$
360	$8.78 \pm 0.37^{a,x}$	$8.18 \pm 0.67^{a,x}$	$4.94 \pm 0.18^{a,y}$	$8.60 \pm 0.38^{a,x}$	$7.61 \pm 0.44^{a,x}$	$4.97 \pm 0.15^{a,y}$	$9.86 \pm 0.32^{a,x}$	$8.63 \pm 0.64^{a,x}$	$5.82 \pm 0.23^{a,y}$

Table 2). There were no significant differences between the percent bioaccessibility of individual fatty acids (C16:0, C18:1, and C18:2) at any timepoint within the same model. For example, the bioaccessibility of the three fatty acids (C16:0, C18:1, C18:2) in the HGS at the end of the gastric phase (180 min) were 6.38 ± 0.83%, 6.30 ± 0.82%, and 7.44 ± 0.94%, respectively, and there were no significant differences between them ($p > 0.05$). By the end of the gastric and intestinal phase (360 min) the bioaccessibility of all three fatty acids had increased (8.78 ± 0.37%, 8.60 ± 0.38%, and 9.86 ± 0.32%) but there were still no significant differences between them. However, there were significant differences between the bioaccessibility of fatty acids at certain timepoints between models. For example, at the end of the gastric phase (180 min) the bioaccessibility of C18:1 was 6.30 ± 0.82%, in the HGS, which was significantly higher than both the shaking water bath model with gastric juice (4.37 ± 0.34%) and the shaking water bath model with only pH-adjusted water (4.21 ± 0.36%) ($p < 0.05$) (Table 2).

The total lipid content of almonds includes triacylglycerols, phospholipids, and minor contributions of other lipid species such as phytosterols. However, previous researchers have stated that the fat content of almonds is predominantly comprised of esterified fatty acids in the form of triacylglycerols,[1] therefore the total bioaccessibility of fatty acids as reflected in Fig. 2 closely reflects the bioaccessibility of total fat. Specifically, it has been determined by previous workers that the combination of oleic and linoleic acid comprises approximately 90% of total fat in almonds.[51] The compositional data gathered in this study showed that extractable fatty acid comprised 58.76 ± 2.44% of initial almond dry mass (ESI Table 1†). Previous researchers have determined the total fat content of California-grown almonds to be in the range of 54–56%,[51] which is close to the value of percentage of fatty acids found in this study, suggesting that the total fat content of almonds is primarily represented by fatty acids.

Particle breakdown

The Rosin–Rammler model provided a satisfactory fit to the cumulative distribution of particles, with the R^2 value for the fit at each timepoint ≥0.99. x_{50} (mm^2) was significantly influenced ($p < 0.05$) by digestion model, digestion time, and their interaction (Table 3). To correct for minor differences in the value of x_{50} for the initial almond particles used for different digestion timepoints, particle size was also expressed as Δx_{50}, the change in particle size from initial (undigested) particles to digested particles. Δx_{50} was significantly influenced by digestion model, digestion time, and their interaction ($p < 0.05$, Fig. 3). There was a significant decrease in particle size during gastric digestion (15.9 mm^2 to 12.2 mm^2, $p < 0.05$) but only in the HGS. There were no statistically significant differences between the sizes of the initial (undigested) particles used for any of the three digestion models.

The particle size distribution spread parameter b (dimensionless) was significantly influenced by digestion model, digestion time, and their interaction ($p < 0.01$, Table 3). Values of b decreased in the HGS, indicating that the distribution of

Table 3 Parameters of the Rosin–Rammler model (eqn (1)) and particles per gram dry solids. The coefficient of determination (R^2) for the Rosin–Rammler distribution fit to the cumulative distribution of particle sizes was ≥0.99 in all cases. All values are means (n = 3) ± standard deviation. Values in each column with no letter in common (abc) represent significant differences (p < 0.05) within a certain model across different digestion times. Values in each row with no letter in common (xyz) represent significant differences (p < 0.05) at a certain digestion time across the different models for each parameter. If no letter is listed, there were no significant differences

	x_{50} (mm^2)			b (dimensionless)			Particles per gram dry solids		
Time (min)	HGS	Shaking water bath	Shaking water bath with only pH adjusted water	HGS	Shaking water bath	Shaking water bath with only pH adjusted water	HGS	Shaking water bath	Shaking water bath with only pH adjusted water
0	15.89 ± 0.68^{a}	15.33 ± 0.17^{b}	16.15 ± 0.28^{c}	2.72 ± 0.10^{a}	2.57 ± 0.03	2.83 ± 0.02	97.5 ± 5.3^{abc}	109.7 ± 10.3^{a}	97.8 ± 4.4^{a}
1	17.62 ± 0.38^{a}	18.40 ± 0.52^{ab}	16.73 ± 1.38^{bc}	2.80 ± 0.12^{a}	2.93 ± 0.13^{a}	2.92 ± 0.27	60.1 ± 1.3^{e,xy}	54.8 ± 1.2^{e,y}	65.8 ± 7.0^{bc,x}
5	17.65 ± 1.03^{a}	18.01 ± 0.03^{ab}	18.45 ± 1.84^{abc}	2.64 ± 0.10^{a}	2.86 ± 0.27^{a}	2.88 ± 0.36	67.7 ± 6.3^{de}	61.7 ± 2.8^{de}	59.4 ± 8.8^{c}
15	16.63 ± 1.03^{a}	18.78 ± 1.75^{a}	17.96 ± 1.92^{abc}	2.52 ± 0.13^{a}	2.78 ± 0.24^{ab}	2.77 ± 0.12	78.7 ± 10.9^{cd}	66.8 ± 12.6^{cde}	65.1 ± 7.8^{bc}
30	15.92 ± 0.91^{a,y}	19.78 ± 1.07^{a,x}	17.85 ± 1.89^{abc,xy}	2.36 ± 0.21^{ab,y}	2.87 ± 0.24^{a,x}	2.60 ± 0.15^{xy}	88.4 ± 15.8^{bcd,x}	61.1 ± 1.5^{de,y}	68.5 ± 7.5^{bc,y}
180	12.19 ± 1.29^{b,y}	18.84 ± 0.71^{a,x}	20.36 ± 1.43^{a,x}	2.00 ± 0.14^{b,y}	2.81 ± 0.21^{ab,x}	2.84 ± 0.07^{x}	156.2 ± 26.9^{ab,x}	74.1 ± 5.2^{bcd,y}	63.8 ± 7.4^{bc,y}
185	12.34 ± 1.53^{b,y}	19.68 ± 1.86^{a,x}	18.98 ± 1.02^{abc,x}	2.01 ± 0.01^{b,y}	2.56 ± 0.26^{ab,x}	2.88 ± 0.11^{x}	172.2 ± 47.7^{ab,x}	69.9 ± 9.0^{bcd,y}	72.6 ± 3.7^{ab,y}
195	11.47 ± 1.49^{b,y}	18.52 ± 1.19^{ab,x}	19.66 ± 0.27^{ab,x}	2.03 ± 0.09^{b,y}	2.52 ± 0.04^{ab,x}	2.85 ± 0.05^{x}	203.2 ± 50.2^{a,x}	81.0 ± 10.1^{abc,y}	66.2 ± 3.5^{bc,y}
360	11.50 ± 2.18^{b,y}	18.42 ± 1.20^{ab,x}	18.57 ± 0.71^{abc,x}	1.93 ± 0.17^{b,z}	2.37 ± 0.16^{b,y}	2.81 ± 0.14^{x}	216.2 ± 47^{a,x}	87.6 ± 10.4^{ab,y}	75.6 ± 1.4^{ab,y}

Fig. 3 Change in Rosin–Rammler x_{50} (eqn (1)) at each timepoint from x_{50} of the initial almond particles subjected to *in vitro* digestion shown for Human Gastric Simulator (●), shaking water bath (▲), and shaking water bath with only pH-adjusted water (■) models. All points represent the mean (n = 3) ± standard deviation.

particles became broader as time elapsed. For example, the value of b decreased from 2.72 ± 0.10 for undigested particles to 2.00 ± 0.14 for particles at the end of the gastric phase (p < 0.01). There were no statistically significant differences between the b values of the initial (undigested) particles used for any of the three digestion models.

The number of particles per gram of dry solids was significantly influenced by digestion model, digestion time, and their interaction (p < 0.01, Table 3). In the HGS, the number of particles per gram increased during digestion, with 60.1 ± 1.3 particles per gram dry solids after one minute of digestion and 216.2 ± 47 particles per gram of dry solids after gastric and intestinal digestion (p < 0.05). After 30 min digestion time the number of particles per gram dry solids was significantly higher in the HGS (88.4 ± 15.8) than in the shaking water bath model with gastric juice (61.1 ± 1.5) or the shaking water bath model with only pH-adjusted water (68.5 ± 7.5), p < 0.05. For all timepoints after 30 min the number of particles per gram dry solids was highest in the HGS, and there were no significant differences between the number of particles per gram dry solids between the two shaking water bath models. There were no statistically significant differences between the particles per gram of dry solids values of the initial (undigested) particles used for any of the three digestion models. Overall, the HGS was the only model that experienced a significant decrease in particle size as represented by Rosin–Rammler x_{50} as well as a significant increase in the number of particles per gram dry solids.

Brix of liquid phase and moisture content of solid phase

°Brix of the liquid digesta was significantly influenced by digestion model, digestion time, and their interaction (p < 0.01, Table 4). Within each model, °Brix was significantly

Table 4 Moisture content of solid particles (g moisture per g dry matter) and °Brix of liquid digesta. All values are means (n = 3) ± standard deviation. Values in each column with no letter in common (abc) represent significant differences ($p < 0.05$) within a certain model across different digestion times. Values in each row with no letter in common (xyz) represent significant differences ($p < 0.05$) at a certain digestion time across the different models. If no letter is listed, there were no significant differences

	°Brix			Moisture content (g moisture per g dry matter)		
Time (min)	HGS	Shaking water bath	Shaking water bath with only pH adjusted water	HGS	Shaking water bath	Shaking water bath with only pH adjusted water
1	0.40 ± 0.06^{c}	0.34 ± 0.03^{d}	0.38 ± 0.07^{e}	$30.72 \pm 4.94^{c,y}$	$35.02 \pm 1.60^{d,xy}$	$42.69 \pm 3.78^{c,x}$
5	0.57 ± 0.15^{c}	0.50 ± 0.03^{c}	0.53 ± 0.03^{e}	37.78 ± 3.40^{c}	40.40 ± 2.86^{d}	45.57 ± 2.45^{c}
15	$1.20 \pm 0.21^{b,x}$	$1.09 \pm 0.23^{b,xy}$	$0.94 \pm 0.05^{d,y}$	$50.05 \pm 4.17^{b,y}$	$54.0 \pm 1.66^{c,xy}$	$61.61 \pm 2.77^{b,x}$
30	$1.41 \pm 0.14^{b,x}$	$1.33 \pm 0.03^{b,x}$	$1.06 \pm 0.11^{cd,y}$	$57.56 \pm 3.40^{b,y}$	$60.59 \pm 6.20^{c,y}$	$71.05 \pm 4.24^{b,x}$
180	$3.05 \pm 0.06^{a,x}$	$3.10 \pm 0.13^{a,x}$	$2.23 \pm 0.04^{a,y}$	$81.89 \pm 6.50^{a,y}$	$89.83 \pm 2.62^{b,x}$	$95.56 \pm 6.27^{a,x}$
185	$2.84 \pm 0.11^{a,x}$	$2.65 \pm 0.08^{a,x}$	$1.17 \pm 0.21^{bcd,y}$	$86.59 \pm 3.23^{a,y}$	$90.23 \pm 0.95^{b,y}$	$98.24 \pm 6.47^{a,x}$
195	$3.01 \pm 0.07^{a,x}$	$2.68 \pm 0.07^{a,x}$	$1.28 \pm 0.11^{bc,y}$	$90.23 \pm 5.68^{a,y}$	$99.18 \pm 4.50^{ab,x}$	$103.72 \pm 3.91^{a,x}$
360	$3.21 \pm 0.00^{a,x}$	$2.85 \pm 0.03^{a,x}$	$1.38 \pm 0.04^{b,y}$	$91.47 \pm 1.21^{a,y}$	$101.83 \pm 1.98^{a,x}$	$104.30 \pm 2.31^{a,x}$

influenced by time ($p < 0.01$). For example, in the HGS °Brix increased from 0.40 ± 0.06 at the 1 min timepoint to 3.05 ± 0.06 at the end of the gastric phase (180 min), and 3.21 ± 0.00 at the end of the gastric and intestinal digestion (360 min).

Moisture content (% dry basis) of the solid particles was significantly influenced by digestion model and digestion time ($p < 0.01$, Table 4) but not their interaction ($p > 0.05$). Within each model, moisture content significantly increased over time ($p < 0.01$). For example, moisture content (percent dry basis) in the HGS increased from 30.72 ± 4.94 after 1 minute of digestion to 91.47 ± 1.21 after the complete gastric and intestinal digestion.

The pH was recorded and adjusted in each model according to the method described previously, and the measured values are shown in ESI Table 2.†

Scanning electron microscopy images

Images of almond particles obtained using Scanning Electron Microscopy (SEM) are shown in Fig. 4. The particle that was digested in the HGS (Fig. 4A) showed that almond cells located on the surface of the particle had ruptured cell walls. The undigested particle (Fig. 4B) showed lipid bodies adhering to the surface of the particle.

Discussion

Fatty acid bioaccessibility increased with time in both the HGS and shaking water bath models. However, fatty acid bioaccessibility at the end of the gastric phase (180 min) was greater for particles digested in the HGS (6.5%) than for those digested in the shaking water bath (4.5%), $p < 0.05$. The fatty acid bioaccessibility measured in the current study can be compared to the results of previous *in vitro* digestions of almonds. Mandalari *et al.*, (2008)[3] conducted *in vitro* digestion of almond cubes of size 2 mm, which were similar in size to the smallest particles used in the current study. Thus, it was hypothesized that fatty acid bioaccessibility found by Mandalari *et al.*, (2008), (7.6% at the end of simulated gastric digestion) would be higher than the value in the current study. This was supported by the data as the fatty acid bioaccessibility at the end of gastric digestion was 6.5% in the HGS model and

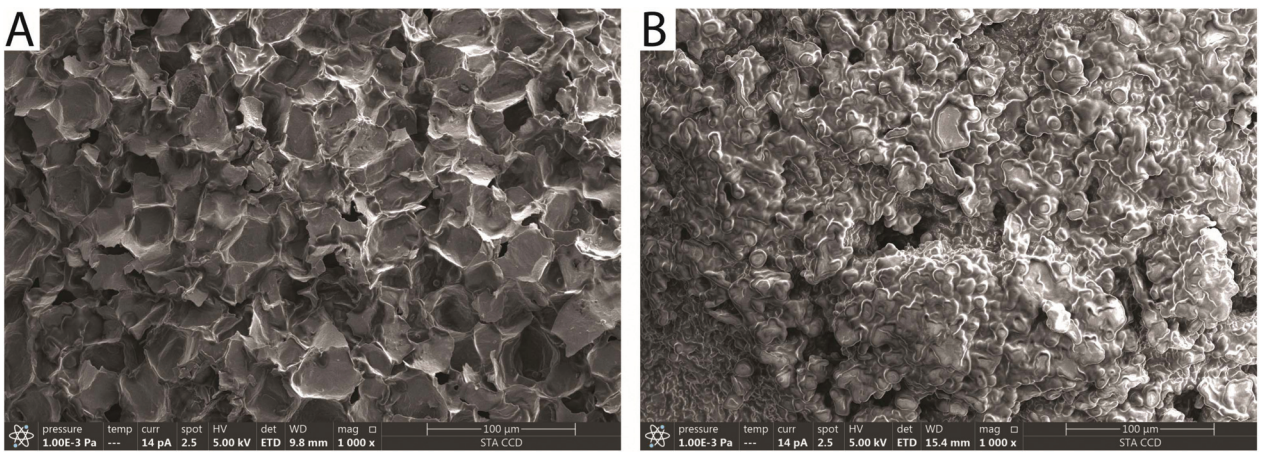

Fig. 4 SEM images of an almond particle that was either (A) digested in the HGS for 180 min; (B) undigested. Scale bars represent 100 µm.

was 4.5% in the shaking water bath model with simulated gastric juice. In another recent study it was found that 8.9% of lipid was released from almond particles after mastication.[52] This is slightly higher than the result from this study (6.5% after gastric digestion in the HGS) which is likely due to the size of almond particles (roughly 1–3 mm) in this previous study, which was smaller than the size of particles in the current study (2–4 mm).

After simulated gastric and intestinal digestion, Mandalari *et al.*, (2008) found fatty acid bioaccessibility of 9.9%. This was slightly higher than the values of fatty acid bioaccessibility in the current study after gastric and intestinal digestion (8.9% in the HGS and 7.9% in the water bath model with simulated gastric juice). The fatty acid bioaccessibility in the HGS was closer to the results of Mandalari *et al.*, (2008), and it is hypothesized that this was due to the particle breakdown which occurred in the HGS but not in the shaking water bath model with simulated gastric juice. Although the initial size of the particles in the HGS and the shaking water bath model with simulated gastric juice were not significantly different, particle breakdown in the HGS effectively made the particles closer in size to those used by Mandalari *et al.*, (2008).

There was a significant reduction in the size of almond particles during the gastric phase in the HGS, but an increase in particle size over time for digestions in the shaking water bath. The increase in particle size in the shaking water bath can be attributed to moisture uptake by almond particles, which also led to increased moisture content. Particle size in the HGS increased from the initial (undigested) timepoint until the 5-minute timepoint, but then began to decrease. This suggests that the magnitude of the particle size reduction in the HGS in the first five minutes of digestion was offset by the simultaneous effect of particle swelling due to moisture uptake. These results were similar to the results of Chen *et al.* who conducted *in vitro* digestion of peanut particles and found an increase in particle size during the first half hour of digestion, followed by a reduction in particle size by the end of the first hour.[20] This supports the findings in the current study and suggests that near the beginning of digestion the change in particle size for nuts can be marked by an increase due to swelling followed by a decrease due to particle breakdown at later timepoints. These results are also supported by the conclusions of a recent study where microscopy was conducted on fecal samples from digestion of natural almonds *in vivo*. In this study, it was determined that the release of lipid during digestion could be in part due to the breakdown of almond particles in the digestive system.[52] Results from the current study provide evidence that some of this breakdown could occur during gastric digestion.

The finding that almond particles broke down during the gastric phase of digestion in the HGS is in contrast to the results of Mandalari *et al.*, (2014) who conducted *in vitro* digestion of masticated almond particles using a dynamic gastric model and reported no significant change in the particle size distribution during digestion.[15] However, the particles used by Mandalari *et al.*, (2014) (mean particle size ~500 μm) were smaller than those used in the current study (2–4 mm) and thus may have been less susceptible to breakdown. This is supported by the results of Chen *et al.* who conducted *in vitro* digestion using peanut particles of size 1–2 mm and reported size reduction of particles initially larger than 1 mm.[20] It has been proposed that larger particles may be more susceptible to breakdown in the gastric environment than smaller particles.[53,54] Overall, the results of the current study, Chen *et al.*,[20] and Mandalari *et al.*, (2014)[15] support this hypothesis, and suggest that nut particles greater than roughly 1 mm in size experience breakdown during *in vitro* gastric digestion in models that simulate the mechanical motion of the human stomach. In human digestion, gastric sieving results in the selective retention of particles larger than roughly 1–2 mm in the stomach.[54,55] Gastric sieving has been reported during *in vivo* digestion of almonds where the growing pig was used as a model for the adult human.[21,22] The results of the current study suggest that nut particles greater than 1 mm can be broken down by *in vitro* models which include simulated peristalsis to a sufficiently small size to resemble those that would be emptied from the human stomach. This data could help future researchers design *in vitro* models for testing hypotheses related to gastric emptying, bioaccessibility, or satiety. To do this, an increased understanding of the mechanisms of particle breakdown during gastric digestion will be essential.

The breakdown of particles in the current study can be attributed to the peristaltic motion of the HGS, because particles in the shaking water bath model with simulated gastric juice did not break down, or increase in size due to swelling. However, it is unclear whether fluid shear, hydrostatic pressure, or particle–particle grinding was responsible for particle breakdown in the HGS.[53,56] Fracture of foods during mastication has been previously reviewed,[57,58] but investigating the mechanisms of structural breakdown of solid foods in the gastric environment could be a topic for future research. In addition to particle breakdown, increased mixing of digesta could also have led to led to the higher lipid bioaccessibility in the HGS as compared to the shaking water bath models. Stronger mixing of *in vitro* digestion systems has been found by previous researchers to result in faster digestion kinetics.[59] In the current study, mixing could have led to higher fatty acid bioaccessibility by facilitating removal of lipolysis products from the lipid–aqueous interface, improving the access of lipases to triacylglycerol inside ruptured almond cells. Previous research has proposed that the oil–water interface can become crowded with products of lipolysis, particularly monoacylglycerol and free fatty acid, which have a hydrophilic and a hydrophobic moiety and self-orient around oil droplets in a monolayer, hindering the adsorption of digestive enzymes to the substrate.[7,60,61] During almond digestion there are additional amphiphilic species that could contribute to interface crowding, for example phospholipids, which surround oil bodies inside almond cells, as well as oleosins, endogenous almond proteins that stabilize oil bodies.[62] The flow of digesta in the HGS could have helped remove these species from the interface, increasing access of digestive enzymes to the con-

tents of almond cells, and contributing to the increased fatty acid bioaccessibility.

Previous researchers have constructed a mathematical model for the bioaccessibility of fatty acids from almonds.[6] The model assumed that almond particles were cubical with known, constant size, that all fatty acids from the outermost layer of cells became bioaccessible during digestion, and that no fatty acids from interior layers of cells became bioaccessible. The model was defined as:

$$L = \frac{1}{2}\left(\frac{64}{\pi^2}\left(\frac{d}{p}\right) - 8\left(\frac{d}{p}\right)^2 + \frac{4}{3}\pi\left(\frac{d}{p}\right)^3\right) \times 100\% \quad (2)$$

where L is predicted lipid bioaccessibility (% of initial), d is the diameter of almond parenchymal cells (~36 μm), and p is the size of cubical almond particles. The model was evaluated for p = 2 mm and p = 4 mm to reflect the smallest and largest particles initially subjected to *in vitro* digestion in the current study, and the predicted fatty acid bioaccessibility values were 5.7% and 2.9%, respectively. Total bioaccessible fatty acid at the end of the gastric and intestinal digestion was 8.9% in the HGS and 7.9% in the shaking water bath model with simulated gastric juice. The slightly higher bioaccessibility values measured in this study could be due to a partial contribution of fatty acids from cells situated beneath the outermost surface of almond particles.[2,5] In the HGS, the model underprediction can also be attributed to particle breakdown as discussed previously.

Overall, the fatty acid bioaccessibility values found by the current study and previous[2,3,6,19] *in vitro* studies are in agreement with the results of a study using human subjects, where it was found that the absorption of fatty acids from almond particles between 1.7–3.4 mm in size was approximately 10%,[8] which is higher than the values predicted by the theoretical model for particles of this size (6.7% for 1.7 mm particles and 3.4% for 3.4 mm particles). This underprediction could have been due to the breakdown of almond particles during gastric digestion by human subjects. Findings of the current study suggest that particle breakdown can be simulated by dynamic *in vitro* models, resulting in fatty acid bioaccessibility values more comparable to the *in vivo* reality.

SEM images suggested that the surfaces of undigested almond particles were coated in lipid bodies (Fig. 4B), whereas particles digested in the HGS for 180 min (Fig. 4A) had ruptured cell walls and lost their intracellular lipid contents during the digestion. Images of digested particles (Fig. 4A) showed the presence of broken cell walls, similar to SEM images of masticated almond particles obtained by previous researchers.[18] This suggests that during either mastication or grinding in a food processor almond cells located on the surfaces of particles are ruptured, and their intracellular contents contribute to bioaccessible lipids during digestion. In this study, SEM images were used as a follow-up investigation and showed that lipid bodies attached to the surface of almond particles were removed during simulated gastric digestion in the HGS. However, in-depth investigation of the lipid release from almonds during digestion could be made using image analysis techniques applied to SEM images. This is an opportunity for future work that has been suggested by previous researchers.[63]

Another objective of the current study was to determine the effect of simulated gastric and intestinal juices on the bioaccessibility of fatty acids from almond particles. Due to the recalcitrance of almond cells it has been proposed that only fatty acids present in cells that are ruptured during mastication or processing can become bioaccessible.[17,64] However, it is not clear whether fatty acids in ruptured cells can be simply washed away from the solid particles in the presence of water, or whether this release is affected by simulated digestive juices. This was investigated by conducting *in vitro* digestions of almond particles in the shaking water bath model using either simulated gastric and intestinal juices or with only pH adjusted water. Results showed that fatty acid bioaccessibility increased over time in the shaking water bath model with simulated gastric and intestinal juices as well as in the shaking water bath model with only pH-adjusted water (p < 0.01). Furthermore, at the end of the gastric phase of digestion (180 min) there was no significant difference in fatty acid bioaccessibility between the shaking water bath model with simulated gastric juice (4.5%) and the shaking water bath model with only pH-adjusted water (4.4%), p > 0.05. However, fatty acid bioaccessibility at the end of gastric and intestinal (360 min) digestion was higher for the shaking water bath model with simulated gastric and intestinal juices (7.9%) than for the shaking water bath model with only pH-adjusted water (5.2%), p < 0.01. This suggests that fatty acid bioaccessibility was not significantly affected by the presence of simulated gastric juice but was affected by simulated intestinal juice. This finding did not support the hypothesis that fatty acid bioaccessibility at the end of the gastric phase would be higher for the shaking water bath model using simulated gastric juice than the shaking water bath model using only pH-adjusted water. It suggests, however, that in this system fatty acids in ruptured almond cells can become released under immersion in water at gastric pH (1.8) as efficiently as in simulated gastric juice.

The significant difference in bioaccessible fatty acid at the end of the intestinal phase between the shaking water bath model with simulated gastric and intestinal juices and the shaking water bath model using only pH-adjusted water suggests that intestinal juice affects fatty acid bioaccessibility. Additionally, models that used simulated intestinal juice experienced a greater increase in fatty acid bioaccessibility between the last timepoint in the gastric phase (180 min) and the first timepoint in the intestinal phase (185 min). This increase was 6.5% to 8.1% in the HGS, 4.5% to 6.5% in the shaking water bath model with simulated gastric and intestinal juices, and 4.4% to 5.0% in shaking water bath model using only pH-adjusted water (Fig. 2). Although the jump in fatty acid bioaccessibility at the beginning of the intestinal phase cannot be attributed to any single component of simulated intestinal juice, it cannot be attributed to a reduction in

particle size. This is because there was no significant difference in particle size or number of particles per gram of dry solids between the last timepoint in the gastric phase (180 min) and the first timepoint in the intestinal phase (185 min) for any model. Thus, emulsification by bile salts was likely responsible for the acute increase in fatty acid bioaccessibility at the start of the intestinal phase. This suggests that, even at the end of the gastric phase, there was still some fatty acid within ruptured cells or adhered to almond particles which was not fully released into the aqueous digesta until interaction with bile salts.

The fatty acids that were quantified in this study may have important functional roles *in vivo*.[65] Compositional data gathered in this study indicated that 93% of fatty acids extracted from almonds were comprised of unsaturated fatty acids (71.7% oleic acid, 21.1% linoleic acid, ESI Table 1†). Results of randomized controlled trials have suggested that individuals adhering to diets including nuts or olive oil had reduced risk factors for cardiovascular events.[12,66] Furthermore, the high ratio of oleic acid to linoleic acid in almonds could be desirable for some consumers, with preliminary evidence suggesting that a higher ratio of oleic to linoleic acid is associated with reduced risk of obesity.[67]

Conclusions

Almond particles broke down in the HGS as evidenced by a significant reduction in particle size and a significant increase in the number of particles per gram of dry solids during the gastric phase. Particle breakdown was attributed to the peristaltic motion of the stomach as it did not occur for *in vitro* models that lacked peristaltic motion. Fatty acid bioaccessibility was greater in the HGS at the end of the gastric phase than in the shaking water bath model when identical simulated gastric juice was used, suggesting that the change in particle size contributed to higher fatty acid bioaccessibility. There was no significant difference in fatty acid bioaccessibility at the end of the gastric phase between digestions conducted in the shaking water bath with simulated gastric juice and digestions in the shaking water bath with only pH-adjusted water. However, fatty acid bioaccessibility at the end of the intestinal phase was higher in the shaking water bath model when simulated intestinal juice was used than when the intestinal digestion was carried out using only pH adjusted water.

Opportunities for future work include elucidating the effects of peristaltic motion on particle breakdown in the gastric environment and determining in more detail the mechanisms of fatty acid emulsification in the intestinal phase of digestion. Overall, results of this study showed that *in vitro* digestion of almond particles using a model with simulated peristaltic contractions resulted in particle size reduction and higher fatty acid bioaccessibility than *in vitro* digestion using a model that lacked peristaltic contractions. Results could assist in the design of future *in vitro* models for simulating human digestion as well as in the development of functional foods for targeted fatty acid bioaccessibility.

Abbreviations

HGS	Human gastric simulator
GC-FID	Gas chromatography with flame ionization detection
SEM	Scanning electron microscopy

Conflicts of interest

There are no conflicts of interest to declare.

Acknowledgements

The authors would like to acknowledge the Almond Board of California for generous donation of almonds. The authors would like to acknowledge Dr Scott Strobel his assistance in the SEM work.

References

1 S. Yada, K. Lapsley and G. Huang, A review of composition studies of cultivated almonds: Macronutrients and micronutrients, *J. Food Compos. Anal.*, 2011, **24**, 469–480.
2 M. M. L. Grundy, P. J. Wilde, P. J. Butterworth, R. Gray and P. R. Ellis, Impact of cell wall encapsulation of almonds on in vitro duodenal lipolysis, *Food Chem.*, 2015, **185**, 405–412.
3 G. Mandalari, R. M. Faulks, G. T. Rich, V. Lo Turco, D. R. Picout, R. B. Lo Curto, G. Bisignano, P. Dugo, G. Dugo, K. W. Waldron, P. R. Ellis and M. S. J. Wickham, Release of protein, lipid, and vitamin E from almond seeds during digestion, *J. Agric. Food Chem.*, 2008, **56**, 3409–3416.
4 S. Gallier, S. M. Rutherford, P. J. Moughan and H. Singh, Effect of food matrix microstructure on stomach emptying rate and apparent ileal fatty acid digestibility of almond lipids, *Food Funct.*, 2014, **5**, 2410–2419.
5 M. M. L. Grundy, F. Carrière, A. R. Mackie, D. A. Gray, P. J. Butterworth and P. R. Ellis, The role of plant cell wall encapsulation and porosity in regulating lipolysis during the digestion of almond seeds, *Food Funct.*, 2016, **7**, 69–78.
6 T. Grassby, D. R. Picout, G. Mandalari, R. M. Faulks, C. W. C. Kendall, G. T. Rich, M. S. J. Wickham, K. Lapsley and P. R. Ellis, Modelling of nutrient bioaccessibility in almond seeds based on the fracture properties of their cell walls, *Food Funct.*, 2014, **5**, 3096–3106.
7 E. Capuano, N. Pellegrini, E. Ntone and C. V. Nikiforidis, In vitro lipid digestion in raw and roasted hazelnut particles and oil bodies, *Food Funct.*, 2018, **9**, 2508–2516.
8 S. E. E. Berry, E. A. Tydeman, H. B. Lewis, R. Phalora, J. Rosborough, D. R. Picout and P. R. Ellis, Manipulation of lipid bioaccessibility of almond seeds influences postpran-

dial lipemia in healthy human subjects, *Am. J. Clin. Nutr.*, 2008, **88**, 922–929.

9 S. K. Gebauer, J. A. Novotny, G. M. Bornhorst and D. J. Baer, Food processing and structure impact the metabolizable energy of almonds, *Food Funct.*, 2016, **7**, 4231–4238.

10 J. A. Novotny, S. K. Gebauer and D. J. Baer, Discrepancy between the Atwater factor predicted and empirically measured energy values of almonds in human diets, *Am. J. Clin. Nutr.*, 2012, **96**, 296–301.

11 S. Li, Y. Liu, J. Liu, W. Chang, C. Chen and C.-Y. O. Chen, Almond consumption improved glycemic control and lipid profiles in patients with type 2 diabetes mellitus, *Metabolism*, 2011, **60**, 474–479.

12 R. Estruch, E. Ros, J. Salas-Salvadó, M.-I. Covas, D. Corella, F. Arós, E. Gómez-Gracia, V. Ruiz-Gutiérrez, M. Fiol, J. Lapetra, R. M. Lamuela-Raventos, L. Serra-Majem, X. Pintó, J. Basora, M. A. Muñoz, J. V. Sorlí, J. A. Martínez, M. Fitó, A. Gea, M. A. Hernán and M. A. Martínez-González, Primary prevention of cardiovascular disease with a mediterranean diet supplemented with extra-virgin olive oil or nuts, *N. Engl. J. Med.*, 2018, **378**, e34(1)–e34(14).

13 M. E. Rusu, A.-M. Gheldiu, A. Mocan, L. Vlase and D.-S. Popa, Anti-aging potential of tree nuts with a focus on the phytochemical composition, molecular mechanisms and thermal stability of major bioactive compounds, *Food Funct.*, 2018, **9**, 2554–2575.

14 M. A. Wien, J. M. Sabaté, D. N. Iklé, S. E. Cole and F. R. Kandeel, Almonds vs complex carbohydrates in a weight reduction program, *Int. J. Obes.*, 2003, **27**, 1365–1372.

15 G. Mandalari, M. M.-L. Grundy, T. Grassby, M. L. Parker, K. L. Cross, S. Chessa, C. Bisignano, D. Barreca, E. Bellocco, G. Laganà, P. J. Butterworth, R. M. Faulks, P. J. Wilde, P. R. Ellis and K. W. Waldron, The effects of processing and mastication on almond lipid bioaccessibility using novel methods of in vitro digestion modelling and micro-structural analysis, *Br. J. Nutr.*, 2014, **112**, 1521–1529.

16 B. A. Cassady, J. H. Hollis, A. D. Fulford, R. V. Considine and R. D. Mattes, Mastication of almonds: Effects of lipid bioaccessibility, appetite, and hormone response, *Am. J. Clin. Nutr.*, 2009, **89**, 794–800.

17 P. R. Ellis, C. W. C. Kendall, Y. Ren, C. Parker, J. F. Pacy, K. W. Waldron and D. J. A. Jenkins, Role of cell walls in the bioaccessibility of lipids in almond seeds, *Am. J. Clin. Nutr.*, 2004, **80**, 604–613.

18 M. M. L. Grundy, T. Grassby, G. Mandalari, K. W. Waldron, P. J. Butterworth, S. E. E. Berry and P. R. Ellis, Effect of mastication on lipid bioaccessibility of almonds in a randomized human study and its implications for digestion kinetics, metabolizable energy, and postprandial lipemia, *Am. J. Clin. Nutr.*, 2015, **101**, 25–33.

19 T. Grassby, G. Mandalari, M. M. L. Grundy, C. H. Edwards, C. Bisignano, D. Trombetta, A. Smeriglio, S. Chessa, S. Ray, J. Sanderson, S. E. Berry, P. R. Ellis and K. W. Waldron, In vitro and in vivo modeling of lipid bioaccessibility and digestion from almond muffins: The importance of the cell-wall barrier mechanism, *J. Funct. Foods*, 2017, **37**, 263–271.

20 J. Chen, V. Gaikwad, M. Holmes, B. Murray, M. Povey, Y. Wang and Y. Zhang, Development of a simple model device for in vitro gastric digestion investigation, *Food Funct.*, 2011, **2**, 174–182.

21 G. M. Bornhorst, M. J. Roman, K. C. Dreschler and R. P. Singh, Physical property changes in raw and roasted almonds during gastric digestion in vivo and in vitro, *Food Biophys.*, 2014, **9**, 39–48.

22 G. M. Bornhorst, K. Kostlan and R. P. Singh, Particle size distribution of brown and white rice during gastric digestion measured by image analysis, *J. Food Sci.*, 2013, **78**, E1383–E1391.

23 G. M. Bornhorst, K. C. Drechsler, C. A. Montoya, S. M. Rutherfurd, P. J. Moughan and R. P. Singh, Gastric protein hydrolysis of raw and roasted almonds in the growing pig, *Food Chem.*, 2016, **211**, 502–508.

24 G. M. Bornhorst, M. J. Ferrua and R. P. Singh, A proposed food breakdown classification system to predict food behavior during gastric digestion, *J. Food Sci.*, 2015, **80**, R924–R934.

25 D. Dupont, M. Alric, S. Blanquet-Diot, G. Bornhorst, C. Cueva, A. Deglaire, S. Denis, M. Ferrua, R. Havenaar, J. Lelieveld, A. R. Mackie, M. Marzorati, O. Menard, M. Minekus, B. Miralles, I. Recio and P. Van den Abbeele, Can dynamic in vitro digestion systems mimic the physiological reality? *Crit. Rev. Food Sci. Nutr.*, 2019, **59**, 1546–1562.

26 S. Bellmann, J. Lelieveld, T. Gorissen, M. Minekus and R. Havenaar, Development of an advanced in vitro model of the stomach and its evaluation versus human gastric physiology, *Food Res. Int.*, 2016, **88**, 191–198.

27 M. Minekus, P. Marteaul, R. Havenaar and J. H. J. Huis in't Veld, A Multicompartmental Dynamic Computer-controlled Model Simulating the Stomach and Small Intestine, *ATLA, Altern. Lab. Anim.*, 1995, **23**, 197–209.

28 B. M. McArthur, R. V. Considine and R. D. Mattes, Mastication of nuts under realistic eating conditions: Implications for energy balance, *Nutrients*, 2018, **10**, 710.

29 M. A. Peyron, A. Mishellany and A. Woda, Particle size distribution of food boluses after mastication of six natural foods, *J. Dent. Res.*, 2004, **83**, 578–582.

30 M. J. Roman, B. J. Burri and R. P. Singh, Release and bioaccessibility of β-carotene from fortified almond butter during in vitro digestion, *J. Agric. Food Chem.*, 2012, **60**, 9659–9666.

31 G. M. Bornhorst and R. P. Singh, Kinetics of in vitro bread bolus digestion with varying oral and gastric digestion parameters, *Food Biophys.*, 2013, **8**, 50–59.

32 S. K. Sathe, N. P. Seeram, H. H. Kshirsagar, D. Heber and K. A. Lapsley, Fatty acid composition of California grown almonds, *J. Food Sci.*, 2008, **73**, 607–614.

33 M. Minekus, M. Alminger, P. Alvito, S. Ballance, T. Bohn, C. Bourlieu, F. Carrière, R. Boutrou, M. Corredig,

D. Dupont, C. Dufour, L. Egger, M. Golding, S. Karakaya, B. Kirkhus, S. Le Feunteun, U. Lesmes, A. Macierzanka, A. Mackie, S. Marze, D. J. McClements, O. Ménard, I. Recio, C. N. Santos, R. P. Singh, G. E. Vegarud, M. S. J. Wickham, W. Weitschies and A. Brodkorb, A standardised static in vitro digestion method suitable for food - an international consensus., *Food Funct.*, 2014, **5**, 1113–1124.

34 P. L. Zentler-Munro, B. A. Assoufi, K. Balasubramanian, S. Cornell, D. Benoliel, T. C. Northfield and M. E. Hodson, Therapeutic Potential and Clinical Efficacy of Acid-Resistant Fungal Lipase in the Treatment of Pancreatic Steatorrhoea due to Cystic Fibrosis, *Pancreas*, 1992, **7**, 311–319.

35 L. Sams, J. Paume, J. Giallo and F. Carrière, Relevant pH and lipase for in vitro models of gastric digestion, *Food Funct.*, 2016, **7**, 30–45.

36 E. Abrahamse, M. Minekus, T. Ludwig, G. A. van Aken, B. van de Heijning, J. Knol, N. Bartke, R. Oozeer, E. M. van der Beek and T. Ludwig, Development of the Digestive System—Experimental Challenges and Approaches of Infant Lipid Digestion, *Food Dig.*, 2012, **3**, 63–77.

37 A. C. Pinheiro, M. Lad, H. D. Silva, M. A. Coimbra, M. Boland and A. A. Vicente, Unravelling the behaviour of curcumin nanoemulsions during in vitro digestion: effect of the surface charge, *Soft Matter*, 2013, **9**, 3147–3154.

38 J. R. Malagelada, G. F. Longstreth, W. H. J. Summerskill and V. L. W. Go, Measurement of gastric functions during digestion of ordinary solid meals in man, *Gastroenterology*, 1976, **70**, 203–210.

39 G. M. Bornhorst, S. M. Rutherfurd, M. J. Roman, B. J. Burri, P. J. Moughan and R. P. Singh, Gastric pH Distribution and Mixing of Soft and Rigid Food Particles in the Stomach using a Dual-Marker Technique, *Food Biophys.*, 2014, **9**, 292–300.

40 D. M. Phinney, *Design, construction, and evaluation of a reactor designed to mimic human gastric digestion*, UC Davis, 2013.

41 A. Ye, J. Cui, D. Dalgleish and H. Singh, The formation and breakdown of structured clots from whole milk during gastric digestion, *Food Funct.*, 2016, **7**, 4259–4266.

42 A. Soyer, B. Özalp, Ü. Dalmıs and V. Bilgin, Effects of freezing temperature and duration of frozen storage on lipid and protein oxidation in chicken meat, *Food Chem.*, 2010, **120**, 1025–1030.

43 M. João Ramalhosa, P. Paíga, S. Morais, M. R. Alves, C. Delerue-matos and M. Beatriz Prior Pinto Oliveira, Lipid content of frozen fish: Comparison of different extraction methods and variability during freezing storage, *Food Chem.*, 2012, **131**, 328–336.

44 C. P. Baron, I. V. H. Kjærsgård, F. Jessen and C. Jacobsen, Protein and Lipid Oxidation during Frozen Storage of Rainbow Trout (Oncorhynchus mykiss), *J. Agric. Food Chem.*, 2007, **55**, 8118–8125.

45 A. Jang, D. Kim, K. Sung, S. Jung, H. J. Kim and C. Jo, The effect of dietary α-lipoic acid, betaine, L-carnitine, and swimming on the obesity of mice induced by a high-fat diet, *Food Funct.*, 2014, **5**, 1966–1974.

46 A. Y. Taha, A. H. Metherel and K. D. Stark, Comparative analysis of standardised and common modifications of methods for lipid extraction for the determination of fatty acids, *Food Chem.*, 2012, **134**, 427–433.

47 X. Capó, M. Martorell, C. Busquets-Cortés, A. Sureda, J. Riera, F. Drobnic, J. A. Tur and A. Pons, Effects of dietary almond- and olive oil-based docosahexaenoic acid- and vitamin E-enriched beverage supplementation on athletic performance and oxidative stress markers, *Food Funct.*, 2016, **7**, 4920–4934.

48 Z. Zhang, C. E. Richardson, M. Hennebelle and A. Y. Taha, Validation of a one-step method for extracting fatty acids from salmon, chicken, and beef samples, *J. Food Sci.*, 2017, **82**, 2291–2297.

49 S. A. Strobel, H. B. Scher, N. Nitin and T. Jeoh, In situ cross-linking of alginate during spray-drying to microencapsulate lipids in powder, *Food Hydrocolloids*, 2016, **58**, 141–149.

50 S. A. Strobel, H. B. Scher, N. Nitin and T. Jeoh, Control of physicochemical and cargo release properties of cross-linked alginate microcapsules formed by spray-drying, *J. Drug Delivery Sci. Technol.*, 2019, **49**, 440–447.

51 S. K. Sathe, Solubilization, electrophoretic characterization and in vitro digstibility of almond (Prunus Amygdalus) proteins, *J. Food Biochem.*, 1993, **16**, 249–264.

52 G. Mandalari, M. L. Parker, M. M. Grundy, T. Grassby, A. Smeriglio, C. Bisignano, R. Raciti, D. Trombetta, D. J. Baer and P. J. Wilde, Understanding the effect of particle size and processing on almond lipid bioaccessibility through microstructural analysis: From mastication to faecal collection, *Nutrients*, 2018, **10**, 213.

53 R. G. Lentle, Deconstructing the physical processes of digestion: reductionist approaches may provide greater understanding, *Food Funct.*, 2018, **9**, 4069–4084.

54 Q. Guo, A. Ye, M. Lad, M. Ferrua, D. Dalgleish and H. Singh, Disintegration kinetics of food gels during gastric digestion and its role on gastric emptying: An in vitro analysis, *Food Funct.*, 2015, **6**, 756–764.

55 R. Gopirajah, K. P. Raichurkar, R. Wadhwa and C. Anandharamakrishnan, The glycemic response to fibre rich foods and their relationship with gastric emptying and motor functions: An MRI study, *Food Funct.*, 2016, **7**, 3964–3972.

56 H. Kozu, I. Kobayashi, M. A. Neves, M. Nakajima, K. Uemura, S. Sato and S. Ichikawa, PIV and CFD studies on analyzing intragastric flow phenomena induced by peristalsis using a human gastric flow simulator., *Food Funct.*, 2014, **5**, 1839–1847.

57 C. G. Skamniotis, M. Elliott and M. N. Charalambides, On modeling the large strain fracture behaviour of soft viscous foods, *Phys. Fluids*, 2017, **29**, 121610.

58 C. Swackhamer and G. M. Bornhorst, Fracture properties of foods: Experimental considerations and applications to mastication, *J. Food Eng.*, 2019, **263**, 213–226.

59 S. Dhital, G. Dolan, R. Stokes and M. J. Gidley, Enzymatic hydrolysis of starch in the presence of cereal soluble fibre polysaccharides, *Food Funct.*, 2014, **5**, 579–586.

60 H. Singh, A. Ye and M. J. Ferrua, Aspects of food structures in the digestive tract, *Curr. Opin. Food Sci.*, 2015, **3**, 85–93.
61 S. Gallier and H. Singh, Behavior of almond oil bodies during in vitro gastric and intestinal digestion, *Food Funct.*, 2012, **3**, 547–555.
62 S. Makkhun, A. Khosla, T. Foster, D. J. McClements, M. M. L. Grundy and D. A. Gray, Impact of extraneous proteins on the gastrointestinal fate of sunflower seed (Helianthus annuus) oil bodies: A simulated gastrointestinal tract study, *Food Funct.*, 2015, **6**, 125–134.
63 M. E. Dalmau, V. Eim, C. Rosselló, J. A. Cárcel and S. Simal, Effects of convective drying and freeze-drying on the release of bioactive compounds from beetroot during in vitro gastric digestion, *Food Funct.*, 2019, **10**, 3209–3223.
64 M. M.-L. Grundy, K. Lapsley and P. R. Ellis, A review of the impact of processing on nutrient bioaccessibility and digestion of almonds, *Int. J. Food Sci. Technol.*, 2016, **51**, 1937–1946.
65 P. C. Calder, Functional Roles of Fatty Acids and Their Effects on Human Health, *JPEN, J. Parenter. Enteral Nutr.*, 2015, **39**, 18S–32S.
66 M. de Lorgeril, P. Salen, J. Martin, I. Monjaud, J. Delaye and N. Mamelle, Mediterranean Diet, Traditional Risk Factors, and the Rate of Cardiovascular Complications After Myocardial Infarction, *Circulation*, 1999, **99**, 779–785.
67 A. P. Simopoulos, An Increase in the Omega-6/Omega-3 Fatty Acid Ratio Increases the Risk for Obesity, *Nutrients*, 2016, **8**, 128.

